

# Promptness and Dissipative Capability of Semi-Active Magnetorheological Dampers



**M. Spizzuoco**

*Department of Structural Engineering, University of Naples Federico II, Italy*

**N. Caterino & A. Occhiuzzi**

*Department of Technology, University of Naples Parthenope, Italy*

## SUMMARY:

The experimental analysis of response time and dissipative capability of two prototype magnetorheological (MR) semi-active (SA) dampers is presented herein. This activity has been conducted during a Italian research project on devices manufactured in Germany.

It is shown how the control delays are strongly dependent on the effectiveness of the electric part of the control hardware, generally being less than 10 ms. A detailed report of the response time analysis based on the above experimental data is presented and commented.

The dissipative capacity of the devices is then analyzed under the action of imposed sinusoidal displacements or triangular displacements, investigating a large range of displacement amplitudes, frequencies and feeding currents. Interesting comparisons in terms of energy are drawn between the use of MR damper in a passive (constant current) and in a SA mode (variable current commanded by a control logic).

*Keywords: semi-active control, magnetorheological dampers, energy dissipation, response time*

## 1. INTRODUCTION

Semi-active (SA) structural control is widely considered the prominent emerging technology in the framework of the seismic protection of structures, because it generally exploits dampers whose dynamic properties can be adjusted in a small time interval according to the characteristics of the seismic input or to the instantaneous behaviour of the structure hosting them. The SA devices behave as smart dampers or reactive force generators, according to the kind of control logic adopted to change in real time their mechanical parameters.

The effectiveness of a SA control strongly depends on the operation velocity, i.e. on the magnitude of the unavoidable delays involved in the control chain. Few papers in literature show investigations on the response time of MR dampers suggesting to further analyze this aspect so crucial for a successfully working of such innovative seismic protection technique.

Occhiuzzi et al. (2003) show the results of a wide experimental analysis addressed to the mechanical and response time characterization of a MR damper able to develop a maximum damping force of about 50 kN and to be supplied by a current up to 3 A. Using a energy-based algorithm to command the 'switch off' and the 'switch on' of the damper, they distinguish:

- i) a time delay of the control electronics (from the moment in which the cited algorithm imposes a switch on or a switch off of the damper to the moment when the current inside the coils starts to rise or to fall), that resulted to be always smaller than 3 ms;
- ii) a delay of the electromagnetic circuit (from the end of the previous one to the stabilization of the current into the damper at its nominal value, with a tolerance of 5%), resulted to be almost 7 ms in the on-off phase, and 10 ms in the off-on phase;
- iii) a mechanical delay of the MR damper (from the end of electronic delay to the moment when the damper – its force – starts to adjust its behaviour according to the command received), measured in 3 ms in the on-off phase, and 6 ms in the off-on phase.

Renzi and Serino (2004), after showing the main results of a experimental campaign on a semi-

actively controlled steel frame equipped with MR dampers, analyze the modelling issues of such advanced structures. Among these, they discussed the influence of response delays, with particular reference to those related to the deactivation phase. They distinguish two phases in this switch off process. The first represents the control delay  $\tau_1$  between the occurrence of the deactivation analytical condition (given by the control algorithm) and the actual time of start of the variation of the mechanical parameters: basing on a wide parametric study, they suggest to assume for this delay a value of 4 ms. The second phase represents the time variation of the mechanical parameters from their maximum to their minimum value: this variation is assumed to be linear in time, resulting to be long about 30 ms.

Koo et al. (2006) develop an apposite procedure for the definition and the experimental determination of the response time of MR dampers. Furthermore, they investigate the parameters affecting the response time, i.e. the effect of operating current, piston velocity, and system compliance. The delays are shown to be strongly dependent from the operating current, assuming values between 15 and 55 ms for current respectively set in the interval from 2 to 0.5 A. Cited authors suggest to evaluate a technique for reducing these delays imposing a transient overdrive of the current in the damper, aiming to achieve the desired force at lower currents sooner than how much they shown in the paper. The electronic circuit response time is also measured, as the time needed to reach the desired value of current starting from zero. This results included in the interval 2-12 ms for current respectively varying from 0.5 to 1.5 A.

Yang et al. (2008) analyze the factors affecting the MR response time, suggesting to take them into account for a optimal design of a MR smart structure. Starting from the statement that a MR fluid needs less than 1 ms to pass from a fluid to a semi-solid state once immersed in a magnetic field of a given intensity (Zhu, 2007), they highlight the influence of the inductance of the electromagnet and of the output impedance of the driving electronics on the overall response time of a MR device.

Guan et al. (2009) experimentally investigated the response time of a large-scale MR damper at different velocities (1 to 4 cm/s) and currents (0.0 to 1.2 A), highlighting the electromagnetic response as the predominant factor influencing such delays, also demonstrating that lesser eddy current leads to a speedier response. They define the response time as the time span needed to achieve 63% of the desired total variation of the force in the damper. In each operation condition, it is tested 3 times and average value is obtained. They concluded that, imposing a same stepping magnitude: a) a larger initial current leads to a shorter response time, b) stepping down the current leads to delays longer than under the stepping up, especially for the current decreasing to zero, c) observed response times for stepping up currents are within the interval 160-240 ms, d) a faster piston velocity results in a faster response. The response time of a SA MR damper generally depends on:

- a) the time needed by the power supply to impose a voltage to the circuit;
- b) the time needed to achieve the desired value of the current, according to the corresponding inductance;
- c) the time needed to achieve the corresponding value of the magnetic field;
- d) the time needed by the fluid to react to the change in the magnetic field.

Data reported above seem to strongly disagree, setting the response time of MR dampers in a quite wide range. In fact, the apparent inconsistency is due to the different concepts of response times adopted by the researchers, as some of them measured only item d) above and others measured items b), c) and d) together. Herein a detailed analysis of items a) to d) is presented, starting from the results of a wide experimental campaign conducted at the laboratory of the University of Naples (Italy) Federico II on two prototype MR dampers manufactured by Maurer Söhne (Munich, Germany).

The experimental tests allowed also to analyze the mechanical behaviour and the dissipation capacity of MR devices, when simple imposed displacement laws were applied by varying the amplitude and frequency of displacement and the current inside the damper. This analysis is herein conducted in terms of dissipated energy as well as in terms of equivalent linear viscous damping.

Interesting considerations have been drawn experimentally comparing the capability to dissipate energy exhibited by the same MR damper when operating as passive device (constant current during the whole test) or in a SA configuration (variable current according to a simple control algorithm). The “semi-active” MR damper resulted to dissipate always more energy than the “passive” one, because the control logic adopted to drive the MR damper during the SA tests forces the device to dissipate energy in optimally selected time intervals.

## 2. EXPERIMENTAL ACTIVITY

Table 2.1 briefly describes the type and number of tests conducted within the above research program. For each of the nine groups the table specifies the type and the number of tests belonging to, the type and characteristics of the imposed displacement law, type of condition determining a ‘switch on’ or a ‘switch off’, and type of operation of the power supply (current-driven or voltage-driven scheme).

**Table 2.1.** Tests performed on MR dampers

Group	Type	No. of tests	Displac. Law	Current, frequency or velocity and displacement amplitude	ON/OFF when	Power supply driven by
I	passive	60	harmonic	$i=0, 0.9, 1.8, 2.7$ A $f=0.5, 1.5, 3$ Hz - $d=10, 20$ mm	-	current
II	passive	60	constant velocity	$i=0, 0.9, 1.8, 2.7$ A $v=0.1, 0.2, 0.3$ m/s - $d=10, 20$ mm	-	current
III	promptness	9	harmonic	$i=1.0, 2.0, 3.0$ A $f=1.5, 3$ Hz - $d=10, 20$ mm	$x = 0$	current
IV	promptness	9	harmonic	$i=1.0, 2.0, 3.0$ A $f=1.5, 3$ Hz - $d=10, 20$ mm	$x = 0$	voltage
V	promptness	9	harmonic	$i=1.0, 2.0, 3.0$ A $f=1.5, 3$ Hz - $d=10, 20$ mm	$\dot{x} = 0$	current
VI	promptness	20	constant velocity	$i=1.0, 2.0, 3.0$ A $v=0.1, 0.2, 0.3$ m/s - $d=10, 20$ mm	$x = 0$	current
VII	passive	60	harmonic	$i=1.0, 2.0, 3.0$ A $f=1.5, 3$ Hz - $d=10, 20$ mm	-	current
VIII	promptness	18	constant velocity	$i=1.0, 2.0, 3.0$ A $v=0.1, 0.2, 0.3$ m/s - $d=10, 20$ mm	$x = 0$	current
IX	semi-active	9	harmonic	$i=1.0, 2.0, 3.0$ A $f=1.5, 3$ Hz - $d=10, 20$ mm	$F_d \cdot \dot{x} > 0$	current

Tests belonging to groups I to VI have been performed using the experimental configuration of the left side of Fig. 2.1, the remaining ones (VII to IX) with the setup of the right side of Fig. 2.1, i.e. the one obtained substituting the rigid steel tubes of the first scheme with elastic springs of stiffness 500 kN/m each, connected in parallel, simulating a linear elastic bracing system. The groups of promptness tests (III–VII) were planned to estimate the time delays of the control chain and then to verify the rapidity of the semi-active system involving the MR device:

- During the tests of groups III and VI, a simple algorithm commanded a ‘switch on’ of the damper (current from zero to 1, 2 or 3 A) and a ‘switch off’ (from 1, 2 or 3 A to 0 A), alternatively, each time the sign of the imposed displacement changed, i.e. at each zero of the damper’s displacement.
- During the tests of group V, a different algorithm commanded a ‘switch on’ of the damper and a ‘switch off’, alternatively, at each zero of the damper’s velocity  $\dot{x}$ .
- The tests of group VIII were based on the use of the same algorithm of tests of group VI but performed using the elastic springs rather than the tubes.
- The tests of group IV were performed like those of group III but the power supply was operated according to a voltage-driven scheme rather than a current-driven one.

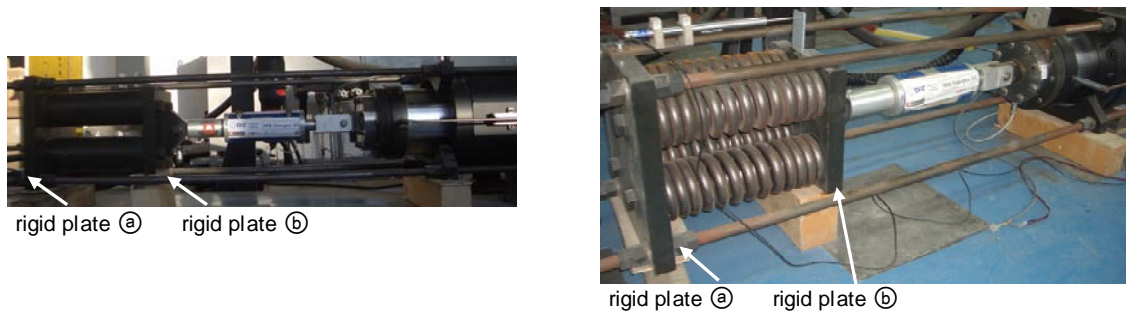


**Figure 2.1.** Experimental configuration with four rigid tubes connecting two rigid plates (left); configuration with four elastic springs between the rigid plates (right)

### 3. RESPONSE TIME OF SEMI-ACTIVE PROTOTYPE MR DAMPERS

The promptness of a semi-active magnetorheological damper is strongly dependent on the time needed to achieve the desired value of the current, and on the time needed by the fluid to react to the change in the magnetic field. The time needed to modify the current, in particular, is closely related to operations of the power supply. In a voltage-driven scheme, the power supply provides a fixed voltage and the current slowly modifies until it reaches a value corresponding to the ratio voltage/resistance. In a current-driven scheme, the power supply provides a fast changing voltage spike so as to quickly modify the current inside the damper. In other words, if the current must be increased, the power supply provides for a short period a voltage spike and then sets the voltage to the reference value, whereas if the current must be decreased, a negative spike of voltage is issued. A power supply having the capability of current-driven operation is referred to as a ‘power-source–power-sink’.

The electrical response time of the SA MR dampers tested by the authors has been measured herein as follows. A command signal  $V_{com}$  is generated by a National Instruments CPU and sent to the device’s power supply, which, in turn, sends a voltage  $V$  to the ends of the damper in order to establish a continuous current of intensity  $i$ . Both the current-driven and voltage-driven approaches are considered, in order to make comparisons among the consequences in terms of the promptness they involve. The main differences of the two different schemes are shown in Fig. 3.1 and 3.2. Diagram 3.1(a) refers to the voltage-driven scheme and corresponds to a ‘switch on’ (0 A  $\rightarrow$  2 A) and the successive ‘switch off’ (2 A  $\rightarrow$  0 A) of the damper. Diagram 3.1(b) refers instead to the current-driven approach, corresponding to a ‘switch on’ and the subsequent ‘switch off’, intended as before. With reference to Fig. 3.1(a), it can be observed that when  $V_{com}$  goes from 0 to 1.5 V, the voltage  $V$  given by the power supply to the damper instantaneously varies from 0 to approximately 8 V, whereas the current  $i$  slowly increases from 0 to 2 A, due to the electric inductance of the coils inside the damper, taking about 215 ms to reach the desired value. Fig. 3.1(a) also shows that the time needed by the current in an on $\rightarrow$ off switch is somewhat longer than 220 ms. In the current-driven operations,  $V_{com}$  is generated in the range 0–5 V. Fig. 3.1(b) shows that when  $V_{com}$  goes from 0 to 5 V, after about 1 ms the voltage sent by the power supply to the damper reaches a spike of about 50 V which lasts about 6 ms, i.e. the time needed by the current to increase from zero to the desired value. After this time, the voltage generated by the power supply falls down to the steady-state value of about 8 V. Fig. 3.1(b) also shows that in current-driven operations, when  $V_{com}$  varies from 5 to 0 V, after about 1 ms the voltage generated by the power supply jumps to  $-50$  V and is kept constant for about 4 ms, which is the time needed for the current to go from 2 to 0 A. After that, the voltage provided by the power supply is kept at a constant value of 0 V. As a conclusion, the electrical response time of SA MR dampers is variable by more than a order of magnitude (5–215 ms) according to the operations and the capabilities of the power supply.

This is clearly highlighted by Fig. 3.2 for three different current levels: 1.0, 2.0 and 3.0 A. It is worth noting that in voltage-driven operations the power requirement is about 16 W, which becomes about 100W in current-driven operations. Therefore, when it is crucial to limit to a few milliseconds the time needed to reach the steady-state phase of the current inside the damper’s electromagnetic circuit, an SA MR damper should be driven by a special power supply according to current-driven operations.

Even if the electrical promptness plays the biggest role (as will be clearly shown in the following), in order to define the global response time of SA control systems based on MR dampers some additional issues should be addressed. In particular, the control chain (acquisition–processing–actuation) of a semi-active system is characterized by the following time delays:

- $\tau_a$ : a time delay of the control electronics which includes, consecutively, the time intervals associated to signal acquisition and processing through the algorithm, the latter being the time interval starting when the algorithm recognizes that a given condition has occurred and ending when the CPU issues a command signal to the power supply;
- $\tau_c$ : a time delay of the power supply, which is the time interval starting when the driving signal (in output from the algorithm and in input to the power supply) is issued and ending when the current (in output from the power supply and in input to the device) begins to change;
- $\tau_e$ : a time delay of the electrical part of the damper, which is the time interval starting when the current (in input to the device) begins to change and ending when the current reaches the commanded nominal value within a  $\pm 5\%$  tolerance;

$\tau_m$ : a time delay of the mechanical part of the damper, representing the time interval between the instant when the current (in input to the device) reaches its nominal value and the instant when the damper begins to react, i.e., begins to adjust its mechanical behaviour.

Therefore, the global response time  $\tau$  has to be assumed equal to the following sum:  $\tau = \tau_a + \tau_c + \tau_e + \tau_m$ . Fig. 3.4 points out the measured time delays during an off→on phase on a magnification of some time-histories recorded during a test performed adopting the current-driven approach, i.e. a imposed harmonic displacement test with frequency 1.5 Hz, amplitude 20 mm and maximum current 2 A. The recorded signals are the displacement imposed by the actuator, the actuator's velocity, the force developed by the device, the driving signal, and the current inside the damper. From Fig. 3.4 it is clear that, regarding the global response time  $\tau$ , the electrical delay  $\tau_e$  causes most of the promptness of the control system based on SA MR dampers. This is confirmed for all the other promptness tests done.

The response times defined above were measured during two on→off phases and two off→on phases in each test, that is, 120 experimental values of  $\tau_a$ ,  $\tau_c$  and  $\tau_e$  were estimated in the case of the current-driven scheme, and 24 measures of the same time delays ( $\tau_a$ ,  $\tau_c$  and  $\tau_e$ ) were taken in the case of the voltage-driven scheme. As regard the mechanical delay of the MR damper  $\tau_m$ , it was not always possible to single out in the force signal the instant when the damper adjusted its mechanical behaviour according to the received command; therefore, the numbers of valid measurements of  $\tau_m$  are 58 and 18, respectively for current-driven and voltage-driven operations.

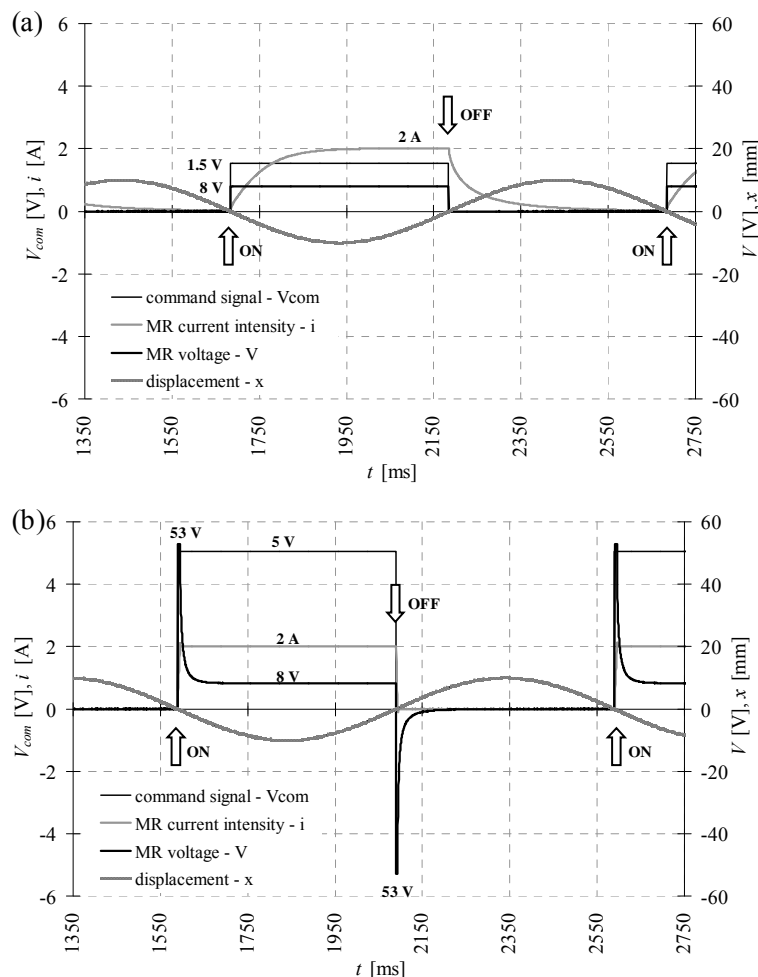


**Figure 3.1.** (a) Voltage-driven MR damper's electrical behaviour when a 'switch on' and a 'switch off' command are issued; (b) current-driven response for a 'switch on' and a 'switch off'

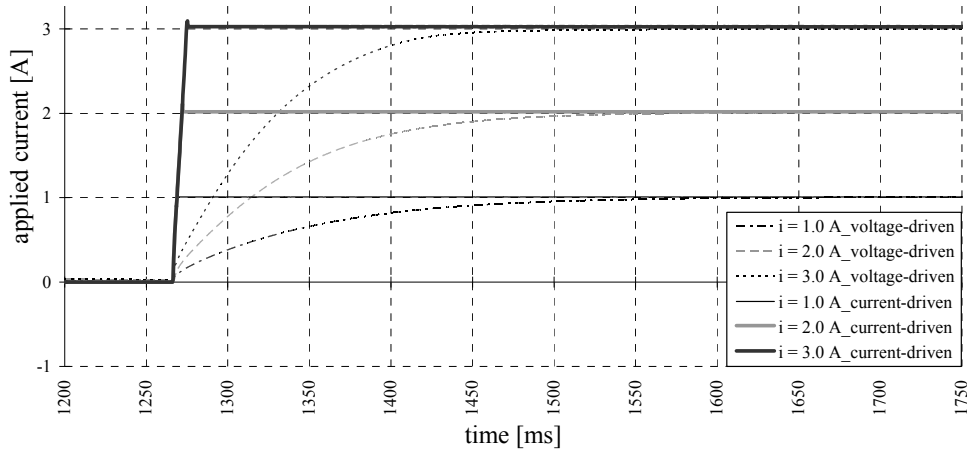


**Figure 3.2.** Circuit response to applied input

The time delays  $\tau_a$  and  $\tau_c$  turned out to be not quite dispersed around 0.4 ms for both the on→off and the off→on phases: their values were not dependent on the maximum commanded current and resulted as rather stable in the many tests performed.

The 120 measures of the time delay  $\tau_c$  at on→off switches are shown in Fig. 3.3(a) as a function of the damper's feeding current, whereas the corresponding 120 determinations at off→on switches are plotted in Fig. 3.3(b), in both cases operating according to the current-driven scheme. The delay  $\tau_c$  of the electromagnetic circuit turned out to be bounded to 6 ms in the on→off switches (Fig. 3.3(a)) and to 9 ms in the off→on ones (Fig. 3.3(b)). The experimental data are moderately scattered around the regression lines shown in Fig. 3.3, which correspond to a quadratic law and to a linear relationship for the on→off and off→on cases, respectively.

The values of the mechanical response time  $\tau_m$ , measured in both the on→off and off→on phases, showed that the response time of the MR fluid turns out to be practically independent of the type of issued command and of the damper's feeding current, leading to an average value of about 1 ms. The promptness tests performed according to the voltage-driven scheme (tests of group IV) yielded values of the time responses  $\tau_a$  and  $\tau_c$  quite close to those found when operating according to the current-driven scheme. Similarly, the mechanical delay  $\tau_m$  was found again to be independent of the command issued by the algorithm and of the damper's feeding current, with an average value of about 1 ms as found before. However, in voltage-driven operations the response time  $\tau_c$  of the electromagnetic circuit is about 20–150 times larger than the one estimated when the power supply is operated according to a current-driven scheme. The 24 measures of  $\tau_c$  in the on→off phases vary in the interval 230–300 ms. The experimental values of  $\tau_c$  in the off→on phases fall in the interval 125–250 ms.

Therefore, it is possible to confirm the fact that the current-driven operations are mandatory for a satisfactory promptness of the system based on MR dampers. Globally, the experimental results described above show that in current-driven operations the time response of an SA MR damper is always less than 8 ms in the on→off phase, and less than 10 ms in the off→on phase.

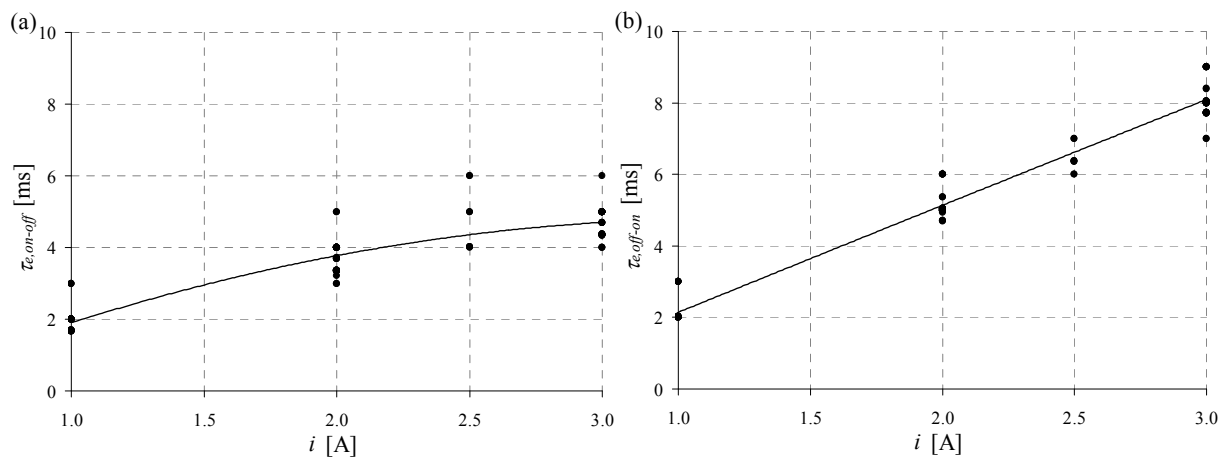


**Figure 3.3.** Measured delays  $\tau_c$  of the current-driven circuit during on→off (a) and off→on phases (b)

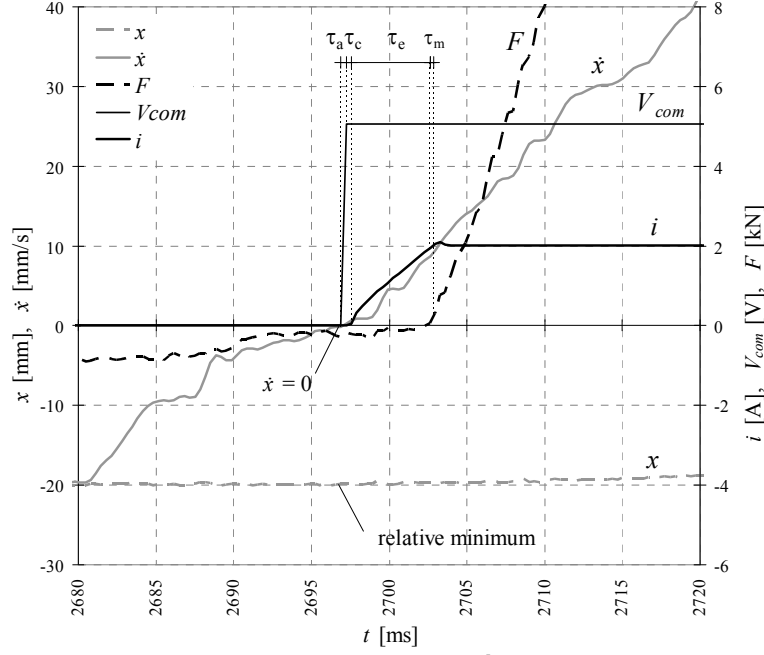


**Figure 3.4.** Promptness of the current-driven MR damper: off→on switch in test at 1.5 Hz, 20 mm and 2 A

#### 4. DISSIPATIVE CAPABILITY OF SEMI-ACTIVELY OPERATING MR DAMPERS

The passive and semi-active experimental tests listed in Table 2.1 have been analyzed in terms of dissipated energy and maximum achieved damper force, in order to draw interesting considerations on the potentiality of a semi-active operation. For each imposed harmonic displacement test of group I, Fig. 4.1(a) shows the energy dissipated in one cycle, while Fig. 4.1(b) plots the energy dissipation occurring in one cycle of all passive imposed constant velocity tests of group II: this energy has been derived as mean value of the dissipated energies during three consecutive cycles. The energy dissipation clearly assumes values increasing with the current level inside the MR damper, and it shows to be nearly independent on the test frequencies and velocities due to the short influence of the fluid viscosity on the global mechanical behaviour of the device. Furthermore, this weak dependence on MR fluid viscosity can be simply deduced by plotting the maximum damper force achieved when the two kinds of displacement law are imposed to the actuator: that is, the MR device develops a maximum force which obviously increases with the feeding current but it is very little variable with the velocity of the test.

For each passive tests of groups I and II, it is possible to derive the viscous damping coefficient of an equivalent linear fluid viscous device which produces approximately the same dynamic response of the investigated MR damper: this equivalence has been evaluated in terms of energy dissipation for the imposed harmonic displacement tests of group I (Fig. 4.2(a)), and in terms of maximum damper force for the imposed constant velocity tests of group II (Fig. 4.2(b)). The damping coefficient of a generic fluid viscous damper can be easily obtained from the expression of the energy dissipated by the device during a single cycle of imposed harmonic motion  $x = d \cdot \sin(2\pi f \cdot t)$ :

$$E_D = \int_0^{2\pi/2\pi f} F_d \cdot \dot{x} dt = \pi \cdot \beta_\alpha \cdot c_\alpha \cdot (2\pi f)^\alpha \cdot d^{\alpha+1} \Rightarrow c_\alpha = E_D / [\pi \cdot \beta_\alpha \cdot (2\pi f)^\alpha \cdot d^{\alpha+1}] \quad (4.1)$$

where  $\alpha$  is the exponent of the damper's velocity  $\dot{x}$  and  $\beta_\alpha = 2^{2+\alpha} \Gamma^2(1+\alpha/2) / [\pi \cdot \Gamma(2+\alpha)]$  is expressed as function of the well known gamma function  $\Gamma(\cdot)$ . In the linear viscous damper case ( $\alpha = 1$ ), the damping coefficient assumes the value  $c_1 = E_D / [\pi (2\pi f) \cdot d^2]$  diagrammed in Fig. 4.2(a) for the tests of group I; in this figure, the maximum velocity achieved during each harmonic displacement test is also indicated ( $v = 0.03$  m/s for a test frequency of 0.5 Hz,  $v = 0.09$  m/s when  $f = 1.5$  Hz, and  $v = 0.19$  m/s for  $f = 3.0$  Hz). On the other hand, the damping coefficient of a linear fluid viscous damper can be simply derived from the maximum experimental force  $F_{max}$  developed during an imposed constant

velocity test, by computing the ratio  $c_1 = F_{max}/v$  (see Fig. 4.2(b) for the tests of group II). It is worth to note that the values of damping coefficient  $c_1$  represented in Fig. 4.2(a) for  $v = 0.09$  m/s and  $v = 0.19$  m/s are very close to those plotted in Fig. 4.2(b) for tests performed at constant velocity  $v = 0.1$  m/s and  $v = 0.2$  m/s, respectively, the current intensity being equal.

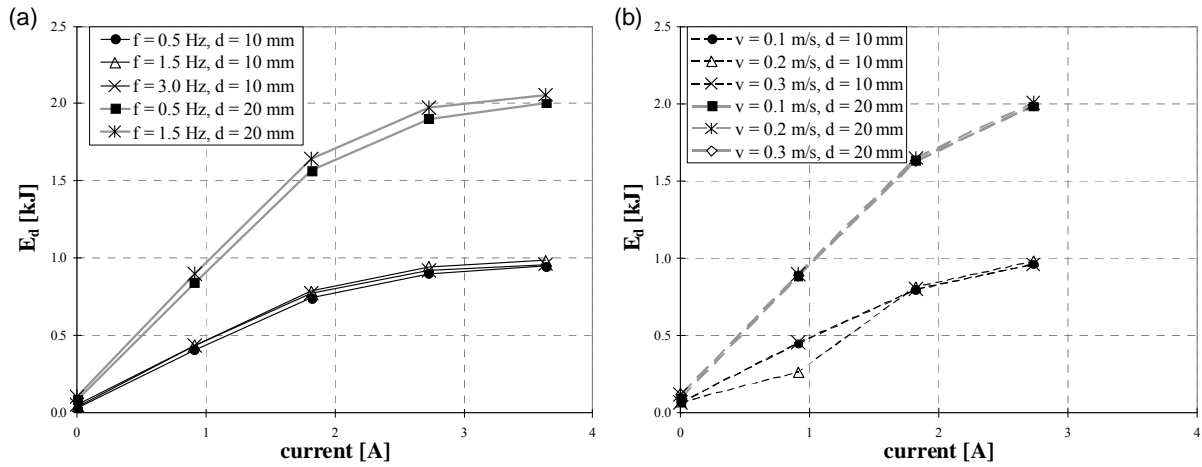


Figure 4.1. Average dissipated energy in one cycle of the tests of group I (a), and group II (b)

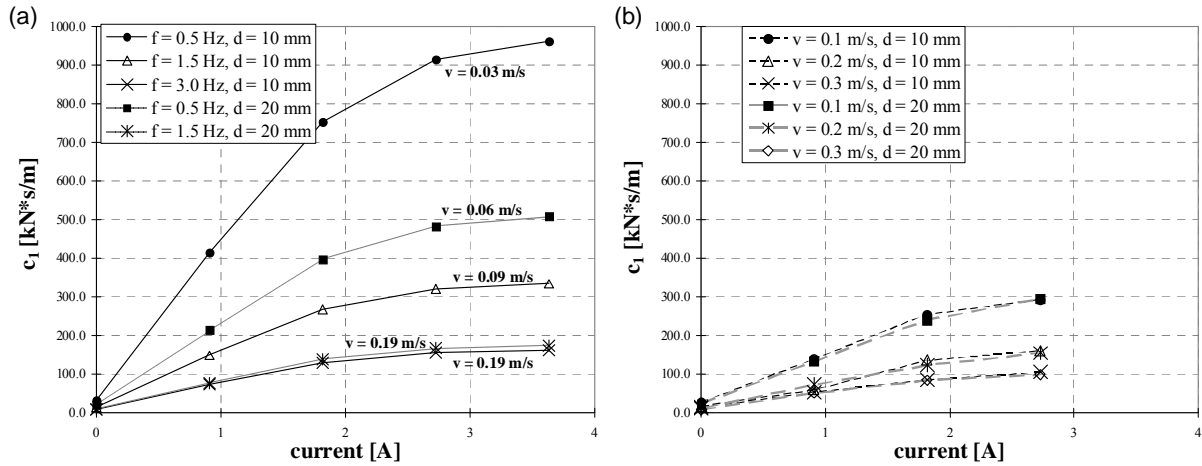
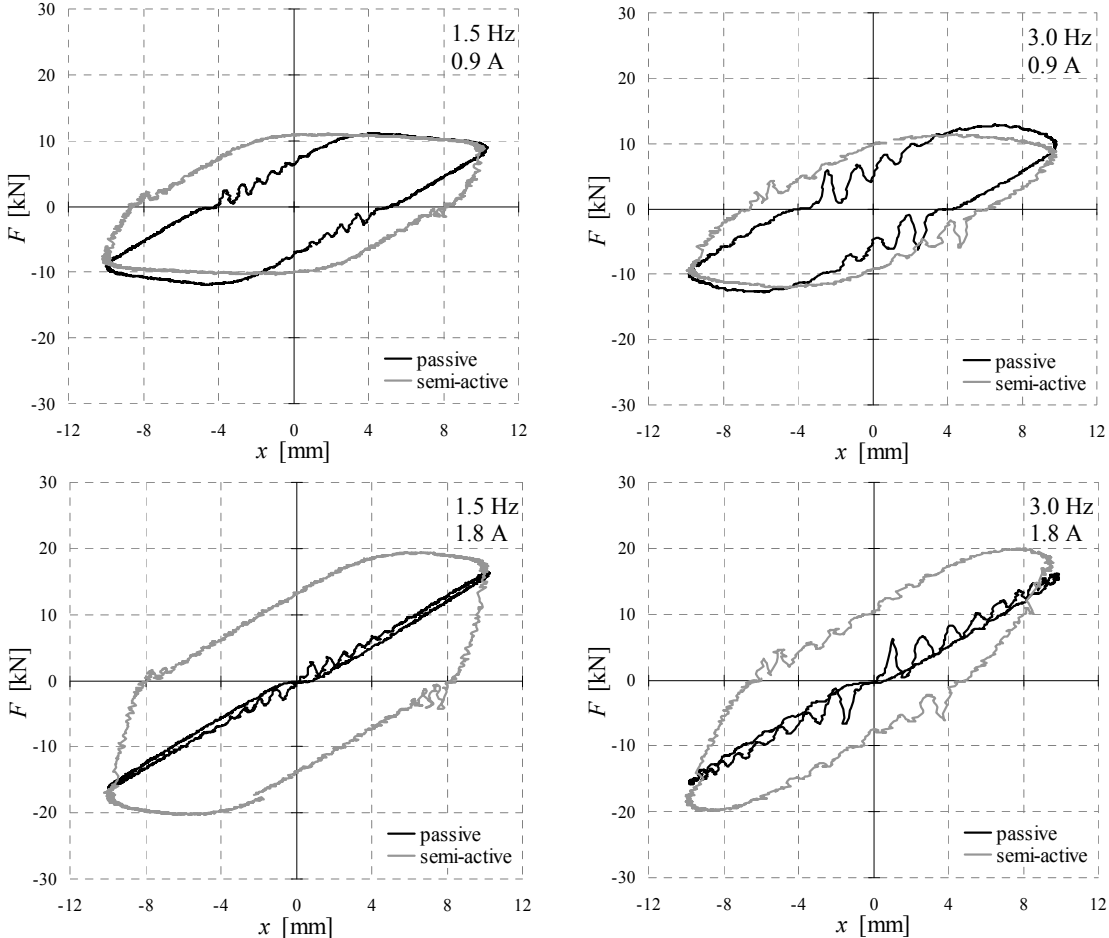


Figure 4.2. Equivalent linear viscous damping from tests of group I (a), and group II (b)

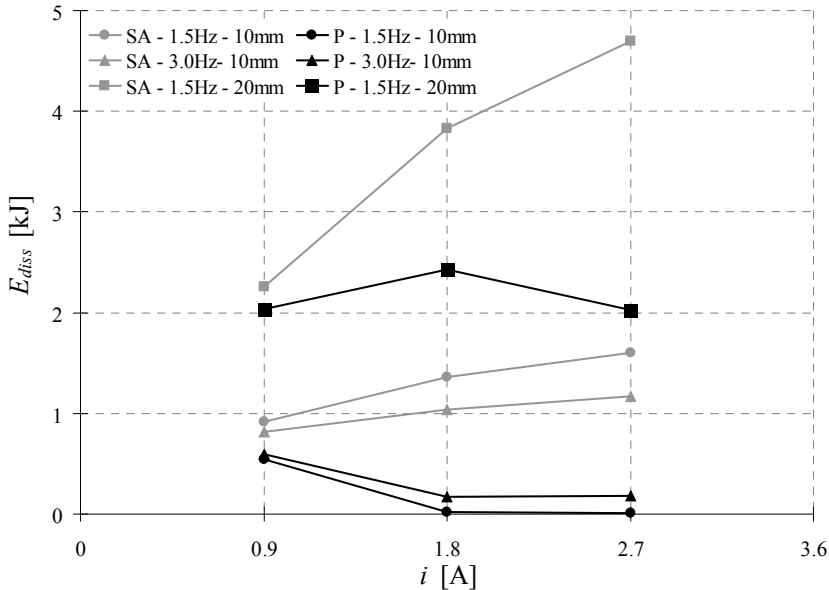
Very interesting results have been deduced by all the tests performed on the experimental configuration represented in the right side of Fig. 2.1. A number of harmonic displacement cycles at constant amplitude were imposed to the damper's piston in order to analyze the dissipation capacity of the assembly, when the MR device is operated both passively (tests group VII) and semi-actively (tests group IX): three different frequencies (0.5, 1.5, 3 Hz) with two different displacement amplitudes (10 and 20 mm) were considered. The semi-active operation was tested by applying an energy-based algorithm, whose physical meaning is that the semi-active bracing system (simulated by the assembly) can temporarily store part of the energy associated to its displacement and then release that energy during fast dissipation processes. The storing phase corresponds to time intervals where the power flowing into the semi-active assembly is positive, i.e. when  $F_d \cdot \dot{x}_f > 0$ : in such storing phase the value of  $F_{dy}$  has to be set as high as possible so as to achieve the maximum possible strain in the elastic springs. On the contrary, when the sign of above product changes to negative, the power flow to the device becomes negative, and the value  $F_{dy}$  has to be switched to its minimum value so as to oblige the MR damper to dissipate the elastic energy stored in the springs in a very short time interval.

Fig. 4.3 compares the experimental cycles of four semi-active tests of group IX with the corresponding passive tests of group VII, while Fig. 4.4 shows the same comparisons by diagramming the amount of energy dissipated by the MR device during one cycle of each passive (P) imposed harmonic displacement test (group VII) and of the corresponding semi-active (SA) test (group IX). The last two

figures clearly make in evidence that the SA MR damper dissipates always more energy than the passive one, because the control logic adopted to drive the MR damper during the SA tests forced the device to dissipate energy in optimally selected time intervals.



**Figure 4.3.** Comparison of semi-active and passive tests in terms of force-displacement cycles, with reference to harmonic displacement tests at 10 mm of amplitude



**Figure 4.4.** Passive vs. semi-active MR damper's dissipation capacity

Fig. 4.4 also shows that the energy dissipated by the SA system increases with the maximum feeding current commanded by the control algorithm, due to the raising of the energy stored in the elastic springs and then released during the dissipation phases, and this increase seems to follow a linear law. Fig. 4.4 also confirms a well-known disadvantage in using passive control systems: the MR device working in the passive mode is able to dissipate an amount of energy which increases up to a certain current level over which the dissipated energy rapidly decreases, because the device results too stiff compared to the springs and the displacement imposed by the actuator is mainly absorbed by the elastic elements. In other words, this result means that a passive MR device, which is fed with a constant current level, can work and dissipate well only when the input excitation is similar to that considered in the design stage, while it can get a much worse performance when the dynamic input is quite different.

## 5. CONCLUSIONS

A wide experimental activity have been conducted on prototype SA MR dampers designed, manufactured and provided by Maurer Söhne (Munich, Germany). It allows to in-depth investigate the dynamic behaviour of magnetorheological dampers. Herein special attention has been paid to the characterization of above dampers in terms of response time and capability to dissipate energy.

The promptness of SA MR devices resulted to be almost exclusively dependent on the effectiveness of the electric part of the control hardware. In particular, operating a SA MR damper in real time requires a power supply with “power source – power sink” capabilities and the adoption of a current-driven control scheme is practically mandatory. Provided that an adequate electric hardware be available and properly tuned, the response time of SA MR dampers is comfortably bounded to 8~10 ms. In many practical applications, this time interval is really short, and thus almost negligible, compared to typical periods of vibration of civil structures. As a consequence, taking explicitly into account the time response of SA MR dampers in control algorithms seems hardly useful.

Experimental tests have been also analyzed to evaluate the amount of dissipated energy, the maximum force exhibited by the damper, and the equivalent linear damping coefficient: they resulted to be strongly dependent from the intensity of current given to the damper, especially for lower values of the latter. The amount of energy dissipated over one cycle of harmonic or constant velocity tests results to be almost independent from the involved working velocities, being (as expected) more strongly related to the magnitude of maximum displacement imposed to the damper.

Finally it has been shown that the dissipative properties of SA MR dampers are much higher than those of their passive counterparts: the control logic driving the SA tests forces the device to dissipate energy in optimally selected time intervals.

## ACKNOWLEDGEMENT

This work has been financially supported by the consortium Reluis on a grant by the Protezione Civile (Italian Emergency Agency). The MR dampers considered in this paper have been designed, manufactured and provided for free by Maurer Söhne (Munich, Germany). Both supports are gratefully acknowledged.

## REFERENCES

- Koo, J.-H., Goncalves, F. D. and Ahmadian, M. (2006). A Comprehensive Analysis of the Response Time of MR Dampers. *Smart Mater. Struct.* **15**, 351-358.
- Renzi, E. and Serino, G. (2004). Testing and modelling a semi-actively controlled steel frame structure equipped with MR dampers. *Journal of Structural Control and Health Monitoring*. **11:3**, 189-221.
- Occhiuzzi, A., Spizzuoco, M. and Serino, G. (2003). Experimental analysis of magnetorheological dampers for structural control. *Smart Materials and Structures*. **12**, 703-711.
- Yang, L., Fubin, D.F. and Eriksson, A. (2008). Analysis of the optimal design strategy of a magnetorheological smart structure. *Smart Material and Structures*, **17**, 8 pp.
- Zhu, C. (2007). The response time of a magnetorheological fluid squeeze film damper rotor system. *Key Eng. Mater.*, vol. 334/335 No. 2, pp. 1085–1088, 2007.
- Guan, X., Guo, P., Ou, J. (2009). Study of the response time of MR dampers, 2nd International Conference on Smart Materials and Nanotechnology in Engineering, Proceedings of SPIE 7493.